Underwater docking of an under-actuated autonomous underwater vehicle: system design and control implementation[*]

Bo LI, Yuan-xin XU[†‡], Shuang-shuang FAN, Wen XU

College of Information Science and Electronic Engineering, Zhejiang University, Hangzhou 310027, China

[†]E-mail: xuyx@zju.edu.cn

Abstract: Underwater docking greatly facilitates and extends operation of an autonomous underwater vehicle (AUV) without the support of a surface vessel. Robust and accurate control is critically important for docking an AUV into a small underwater funnel-type dock station. In this paper, a docking system with an under-actuated AUV is presented, with special attention paid to control algorithm design and implementation. For an under-actuated AUV, the cross-track error can be controlled only via vehicle heading modulation, so both the cross-track error and heading error have to be constrained to achieve successful docking operations, while the control problem can be even more complicated in practical scenarios with the presence of unknown ocean currents. To cope with the above issues, a control scheme of a three-hierarchy structure of control loops is developed, which has been embedded with online current estimator/compensator and effective control parameter tuning. The current estimator can evaluate both horizontal and vertical current velocity components, based only on the measurement of AUV's velocity relative to the ground; in contrast, most existing methods use the measurements of both AUV's velocities respectively relative to the ground and the water column. In addition to numerical simulation, the proposed docking scheme is fully implemented in a prototype AUV using MOOS-IvP architecture. Simulation results show that the current estimator/compensator works well even in the presence of lateral current disturbance. Finally, a series of sea trials are conducted to validate the current estimator/compensator and the whole docking system. The sea trial results show that our control methods can drive the AUV into the dock station effectively and robustly.

Key words: Autonomous underwater vehicle (AUV); Docking systems; Current estimator; Current compensation; Docking control

https://doi.org/10.1631/FITEE.1700382　　　　　　　　**CLC number:** TP242

1 Introduction

Use of autonomous underwater vehicles (AUVs) has much increased in ocean activities in recent years; example applications include military surveillance (Curtin et al., 1993), ecosystem monitoring (Baumgartner et al., 2014), scientific application (Ludvigsen et al., 2014; Zhang et al., 2016), three-dimensional (3D) visual observation (Sato et al., 2014), oil spill detection (Choyekh et al., 2015), and deep-sea exploitation (Kilgour et al., 2014). In such applications, users almost always desire that an AUV can carry more sensors, some of which may be quite power intensive, and be operated for long duration and large coverage (Baumgartner et al., 2014; Zhang et al., 2014; Choyekh et al., 2015). This requirement can hardly be met given the limitation in the state-of-the-art battery technology (Bradley et al., 2001; Borgogna et al., 2015). As a consequence, traditionally AUVs can only survey around the shore or must be accompanied by a support ship (McEwen et al., 2008).

To mitigate the ship support requirements and also increase the covert nature of AUV operations, numerous research groups have developed various

docking technologies (Singh et al., 2001; McEwen et al., 2008; Park et al., 2009; Peng et al., 2014; Li DJ et al., 2015). The basic function of a docking system is to charge the AUV, download data, and upload new missions (McEwen et al., 2008). As the in-situ underwater electricity charging and data transmission techniques improve, docking an AUV becomes practical (Li et al., 2010; Chen et al., 2012a, 2012b; Shi et al., 2014).

Singh et al. (2001) introduced a docking system based upon an acoustic ultra-short baseline (USBL) system that allows the AUV to approach the dock from any direction. The system was installed on the mooring of an autonomous ocean sampling network, and the dock was capable of long-term deployment at a remote site. Allen et al. (2006) presented the design, development, and testing results of the field demonstrations of a funnel-type docking station for a modified REMUS-100 series AUV; a digital USBL system was used to navigate the AUV into the entrance nozzle of the dock. A funnel-type docking system for a torpedo-like flying vehicle was designed, built, and tested at sea by McEwen et al. (2008). The dock was attached to a cabled observatory in southern Monterey Bay, used to support docking operations with a 54-cm diameter AUV; it had a fixed heading, and provided rigid data/power connection and safe parking for the AUV. A vision guided docking system was presented by Park et al. (2009). There are five lights installed on the dock for vision guidance. A funnel-type docking system was introduced by Li DJ et al. (2015). The dock station was connected to a cabled ocean observatory network, which can charge the AUV, download data, and upload new missions. Peng et al. (2014) presented a hybrid glider for underwater docking. A dynamic model of the hybrid glider was derived and evaluated for docking with a funnel-type dock.

Robust and accurate control is critically important for docking an AUV to a small underwater structure, and the problem will become even more complicated with the presence of unknown currents (Cowen et al., 1997; Teo et al., 2012). Cowen et al. (1997) introduced optical terminal guidance for docking, and a traditional proportional–integral–derivative (PID) controller was adopted. The system was shown to be effective without current disturbance. McEwen et al. (2008) proposed a controller for AUV

docking, with the current being considered as a disturbance in the control loop but without the corresponding consideration in the controller design. A conceptual idea to overcome the current effect was introduced by Park et al. (2009), as in this study the current velocity was assumed to be known. Park et al. (2011a, 2011b) presented a time-varying current observer for current velocity estimation, and the performance of the observer was evaluated by simulation. However, in their study the AUV was modeled as a mass particle, and the current observer had less consideration on the actual control response of the vehicle; therefore, the method can hardly be applied in practice. Refsnes et al. (2006) presented a controller using the estimate of the current velocity to compensate for environmental disturbances; however, some theoretical analyses were given without any experimental validation. Teo et al. (2012, 2015) proposed a fuzzy controller for AUV docking control, which took current estimation into consideration. The proposed current estimator could potentially handle unknown ocean currents. However, the estimator required the AUV conduct an open-loop mission at first for current estimation, which is not practical in high sea states or harsh environments and thus could be tested only by simulations. The path-following control for fully actuated and under-actuated vehicles was analyzed by Xiang et al. (2016), indicating that the side-slip angle of the vehicle plays an important role in the evolution of the dynamics with different actuation configurations. Xie et al. (2016) gave a review of the control methods used in spacecrafts, which can be applied for an underwater vehicle. Zhou et al. (2013) presented a neural network method integrating a path-following control algorithm with current disturbance resistance capability, and the controllers were designed to guarantee that all the error states in the path-following system were asymptotically stable. Simulation results illustrated that the proposed methodology was effective and capable of attenuating the path-following error in currents. However, this approach was just implemented by simulation, and the feasibility of implementation in a real system is hard to tell.

This study is focused on the design and implementation of the docking strategy, controller, and current estimator/compensator. A docking system with an under-actuated AUV is presented and the

control strategy is developed for AUV docking with an unknown current. For an under-actuated AUV, special attention should be paid to docking control because the cross-track error can be controlled only via vehicle heading modulation, so both the highly accurate cross-track and heading control are required to ensure successful docking operations, while the control problem can be even more complicated in practical scenarios with the presence of unknown currents. A current estimator for both horizontal and vertical currents is developed based on the AUV control results, which need only the information of the vehicle's velocity relative to the ground. The proposed current estimator requires low sensor configuration, which can reduce cost in practice. A current compensator is also designed and applied in the docking control loop. A robust control strategy for under-actuated AUV docking is further proposed. The control strategy and current estimator are validated via both simulation and sea trials. Through simulation and experiments, the proposed approaches are demonstrated to be effective, and robust in compensating for current disturbances. Besides, the functions of the whole docking system are fully tested during the sea trials.

2 Docking system design

A docking system is designed, including two parts: dock station and docking AUV (Fig. 1). The basic function of our dock station is to charge the AUV, download data, and upload new missions. The docking AUV should have the capability to guide, navigate, and control itself into the dock station in a strategic manner.

2.1 Dock station

The dock station is a funnel-type one, designed to stand on the seafloor and can be connected to a cabled ocean observatory network (Fig. 1). The dock consists of the following parts: funnel-shaped entrance, terminal tube, base, waterproof chamber, USBL, underwater camera, two underwater lights, compass, depth sensor, and data and power transmission components.

The funnel-shaped entrance, with a diameter of 1.2 m and a cone angle of 70°, is used to guide the AUV into the terminal tube. The funnel and tube are
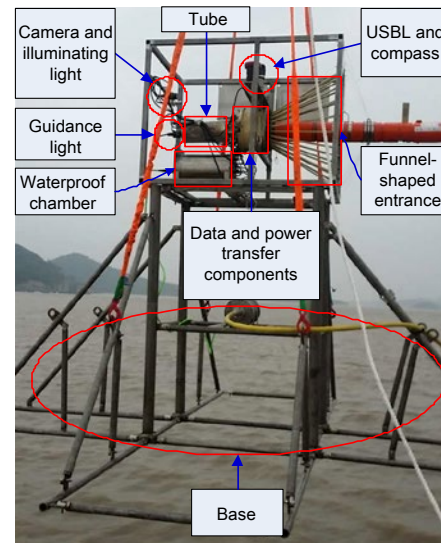

Fig. 1 Photo of the designed docking system

fixed on the top of a 3-m-tall base, and the total weight of the base is about 3500 kg. These parameters are determined by the required docking trial conditions (Shi et al., 2015). The control circuits of the dock station are installed in a waterproof chamber; they are used to manage all the devices installed on the dock station, including all the navigation sensors, observation sensors, and data and power transmission components. A USBL is fixed atop the dock station to locate the AUV and then transmits the location information to the AUV acoustically. Since the location of the dock station is pre-known and the orientation of the dock station can be measured by the compass equipped, the dock information can be sent to the AUV through the USBL periodically. The underwater camera is used to inspect the docking process. The lights on the dock station provide a landmark for AUV vision guidance and can also illuminate the area around, so that the vehicle can be visible through the inspecting camera. The compass measures the dock orientation, and the depth sensor gives the absolute depth of the dock station. The data and power transmission components are applied for data exchange and power charging between the dock station and the AUV. This is the main function of the docking system in Li DJ et al. (2015) for detailed design.

2.2 Docking vehicle

A torpedo-like AUV is used for docking operation. This is a modified version of the Dolphin II AUV developed at Zhejiang University (Li et al.,

2014; Zhang et al., 2014) (Fig. 2). With the front payload customized for docking, the AUV has a length of 2.5 m; the diameter of the standard modules is 200 mm, and for the front docking payload part, the diameter is 290 mm.
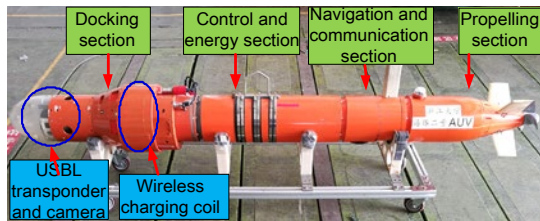

Fig. 2 The modified Dolphin-II AUV for docking

2.2.1 Hardware system

The docking AUV is a modular designed system, consisting of four sections: propulsion section, control and energy section, navigation and communication section, and docking section.

The propulsion section includes one propeller and four control planes, through which the speed and attitude of the AUV can be controlled. An X-shaped control plane structure is adopted to have better maneuverability. The control and energy section consists of the PC104-based control computer and the related peripheral system and a battery pack. The battery is a rechargeable lithium battery, which can be charged by the dock station. The navigation and communication section includes a depth sensor, a compass, and a Doppler velocity log (DVL), which measures AUV's altitude and velocity with respect to the bottom. The radio, WiFi, and Global Position System (GPS) antennas are contained in a 20 cm high antenna housing. The docking section is specially designed to implement docking functions as mentioned above. It includes one acoustic transducer for communication and AUV positioning, one camera for terminal vision guidance, one coil and charging circuits for wireless power charging, and a WiFi antenna for high speed data transmission.

2.2.2 Software system

The modular software development of the AUV is based on MOOS-IvP architecture (Newman, 2008). MOOS stands for 'mission oriented operating suite' and IvP stands for 'interval programming', which is a mathematical programming model for multi-objective optimization.

MOOS has a star topology structure (Fig. 3). A MOOS community consists of processes that communicate through a database process called the MOOSDB in a 'publish and subscribe' manner. Each MOOS process has two key methods, which are called at a user-specified frequency. The OnNew-Mail() is used to check for new mail from the MOOSDB. The Iterate() method is called to allow the process to handle any newly received mail, and the results are then published back to the MOOSDB.
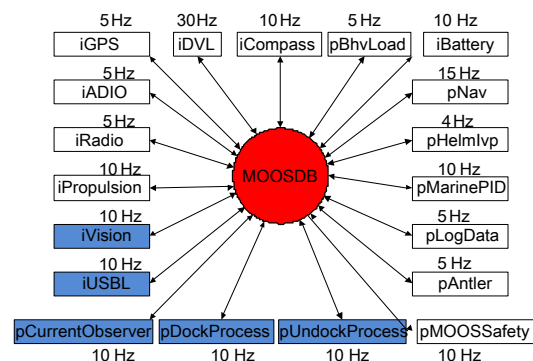

Fig. 3 MOOS community of the docking AUV. Each process is denoted by its name and calling frequency

As shown in Fig. 3, the MOOS community in the docking AUV is composed of processes for navigation (iGPS, iDVL, iCompass, iUSBL, iVision, pNav), control (pMarinePID, pHelmIvp, iADIO), docking operation (pDockProcess, pUndockProcess), propulsion (iPropulsion), energy (iBattery), safety (pMOOSSafety), communication (iRadio), and data log (pLogData). Processes with prefix 'i' are called interface applications, which interact with individual external devices. Processes with prefix 'p' are called pure applications, which process data acquired from MOOSDB. The processes with white background in Fig. 3 are the basic AUV functions. The processes with blue background are especially developed for docking operation. iUSBL and iVision are used for docking guidance. pDockProcess and pUndockProcess are used to implement docking and undocking sequences, respectively. pCurrentObserver is used for online current estimation.

2.3 Docking scheme analysis

The dock station is deployed on the sea floor with position measured a priori. The depth and

orientation of the funnel are measured by the depth sensor and compass installed on the dock station, respectively. The USBL and vision are used for terminal navigation and guidance, respectively, and thus only a rough estimate of the initial location of the dock is needed.

Given the performance of the navigation devices and the control objective, the AUV docking control process is divided into the following steps:

1. Autonomous navigation and waypoint tracking guidance

When the AUV starts homing, it may have been navigated using the measurements of onboard navigation devices but not USBL and GPS. Thus, there will exist some accumulated navigation errors. In the presence of large navigation errors, it is better to make the AUV conduct a waypoint tracking mission to the dock station in order to drive the vehicle to within the USBL range. Based on the lake test results, the USBL signal is good enough within a range of about 150 m.

2. Flying around and searching for USBL signal

If the AUV receives a USBL signal, it fuses the USBL information into the navigation filter to eliminate the accumulated error, and begins to execute step 3. If the AUV did not receive any USBL signal at step 1, it could be that the vehicle is not in the USBL field of view or that the navigation error is too large and thus the vehicle is out of the USBL range. In this case, the AUV will begin to fly around the dock in a circle and search for USBL signals.

3. Going to the marked point

To improve the probability of successful docking, the AUV is driven to arrive at a marked point at first, which is located along the dock centerline and the location is previously determined after the deployment of the dock station. In our test, the point is set 150 m away from the dock station.

4. USBL aided homing guidance and path following

If the AUV reaches the marked point, it will approach along the dock centerline with cross-track error control, aided by USBL navigation information. The USBL can supply signals every 8 s at this step, and the AUV processes the DVL and compass measurements using the extended Kalman filter (EKF) to navigate the vehicle through the gap of USBL updates. The disturbance caused by lateral ocean current will be compensated, and thus the vehicle will not be blown downwind during its approaching. Meanwhile, the vehicle decreases its speed (to 1 m/s in our case) to prevent it from hitting the dock with too much momentum.

5. Terminal computer vision guidance and control

When the AUV is less than 20 m away from the dock, it begins to check the vision signal. If the AUV receives the vision signal, it fuses the information to the control loop. If there is no vision signal, the vehicle will use the USBL signal for docking guidance. This stage is critical for docking operation. Details of the control considerations are given in our previous work (Li B et al., 2015).

6. In dock and latch

The dock station uses a WiFi connection to judge if the AUV has docked with the station successfully; if the WiFi between the AUV and the dock is connected, the docking operation is successful. When the AUV is in dock, the dock control system will power on the electromagnet, which will grip the AUV immediately. Once the AUV is latched, it can start to charge the battery and upload or download data.

In our docking strategy, the conventional 3D path-following problem is divided into motion controls in the horizontal plane and vertical plane separately. This aims to simplify the controller design. Different from most of the existing docking systems, a long-distance straight-path-following strategy is proposed in our docking process, and the advantages are as follows: (1) Docking in a straight path along the dock centerline enables the AUV to estimate the current velocity easily; (2) The AUV moving along the dock centerline can achieve the maximum docking view angles and ensure better acoustic and vision signals; (3) Our docking strategy requires a relatively loose bound on the navigation accuracy compared with the 3D path-following control scheme. In our case, the AUV requires high navigation accuracy across the cone axis but low navigation accuracy along the dock centerline.

The above docking strategy is fully implemented in our AUV prototype using MOOS-IvP architecture. Fig. 4 shows the simplified docking process in state diagram form.

If the vehicle finishes power recharging and the new mission is obtained, the AUV will begin with the undocking process by reversing the propeller. The

distance between the vehicle and the dock is checked to determine whether the vehicle undocks with the dock successfully. If the distance between the dock station and the AUV is large enough, the undocking is considered to be successful. The undocking process is illustrated by Fig. 5.

Each of the operation stage has a timeout judgment during the docking and undocking processes.
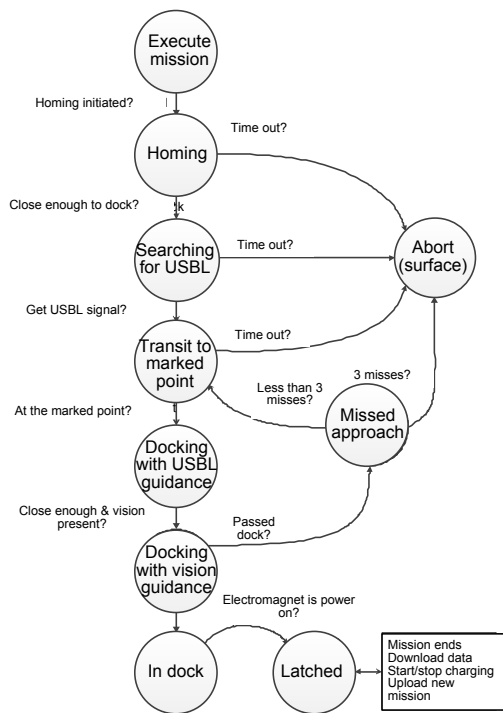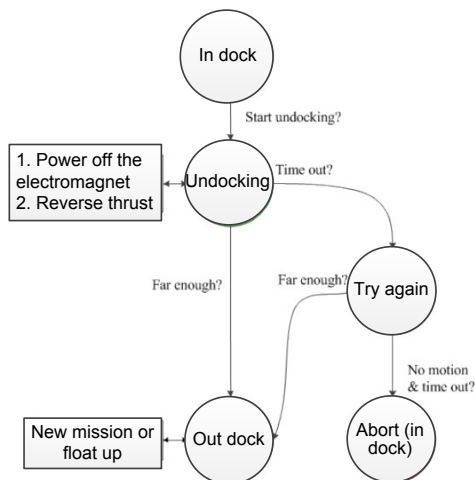

Fig. 4 State diagram of the homing and docking sequence

Fig. 5 State diagram of the undocking process

3 Docking control and current compensator

The primary task in a docking mission is to navigate and control the AUV into the dock station safely. Steps 4 and 5 in Section 2.3 are critically important in the docking operation. For an underactuated AUV, no lateral thruster is used for sway control, and one can control only its heading to eliminate the cross-track error. It is quite challenging, if not impossible, to maintain an AUV heading toward the dock perfectly while maintaining a zero cross-track error under the lateral current disturbance. Thus, the main concern of the docking control is how to eliminate the cross-track error in the presence of lateral current. In this section, mainly the horizontal plane controller in steps 4 and 5 are studied, and a current estimator and a current compensator are designed in addition to the controller.

3.1 Docking control strategy

The control objective is to force the autonomous vehicle to track the docking cone centerline in the presence of lateral current. Here we assume that the forward velocity of the AUV is non-zero, and that the velocity of lateral current remains stable.

Fig. 6 shows the definitions of the symbols in the docking controller design. Angles are defined to be positive clockwise and zero in the north. There are three coordinate systems: Earth-fixed frame, AUV body frame, and dock frame. The dock station is located at $(x_{\text{dock}}, y_{\text{dock}})$, and its orientation is φ_{dock}, both expressed in the Earth-fixed frame. Δy is the cross-track error of the AUV with respect to the dock centerline, Δd is the distance projection between the AUV and the dock along the dock centerline, and $\Delta\psi = \psi_{\text{AUV}} - (\varphi_{\text{dock}} + 180°)$ is the angle between dock heading and AUV heading, called 'cross angle' here. $v_{\text{lateral\_current}}$ is the velocity of the lateral current in the docking frame. A successful docking operation has strict control constraints on Δy and $\Delta\psi$ at the final docking point, which are determined by the dimension of the dock entrance. In our docking system, the control objective is to make $\Delta y < 0.6$ m and $\Delta\psi < 35°$ regardless of the current disturbances. Fig. 7 presents docking control loops in the horizontal plane. There is a three-hierarchy structure of control loops, embedding a current estimator and a current compensator. The outer loop is developed to calculate the cross-

track error and transform the cross-track error Δy to the equivalent heading control angle $\Delta\varphi'$. The middle control loop fuses the equivalent heading control angle φ', current compensation angle $\varphi_{crab\text{-}angle}$, and AUV current heading error $\Delta\psi_{AUV}$ together as the inputs of the inner controller. The inner loop is the basic controller for yaw control, and its outputs are the deflection angles of the control planes. In our docking controller, heading control parameters need to be tuned first, and then the proportional factors of the equivalent heading control angle and crab angle are tuned. The input of the inner control loop is Δe:

$$\Delta e = k_1 \Delta\varphi' + k_2 \varphi_{crab\_angle} + k_3 \Delta\psi_{AUV}, \qquad (1)$$

where k_1, k_2, and k_3 are proportional factors of the above three angles.

Note that

$$\Delta\psi_{AUV} = \psi_{AUV} - \psi_{ref}, \qquad (2)$$

$$\varphi_{crab\_angle} = \arctan\left(\frac{v_{lateral\_currents}}{v_{total}}\right), \qquad (3)$$

where $\psi_{ref} = \varphi_{dock} + 180°$. Since we have defined a cross angle $\Delta\psi$ as mentioned before, here $\Delta\psi_{AUV} = \Delta\psi$. $v_{latreral\_currents}$ is the velocity of the lateral current to be estimated, and v_{total} is the speed of the AUV relative to the ground. A current estimator is integrated in the docking controller (Fig. 7). Before compensating for current disturbance, the AUV is set to work under cross-track error control with $k_2 = 0$ in Eq. (1), to estimate the lateral current velocity. Then the estimated
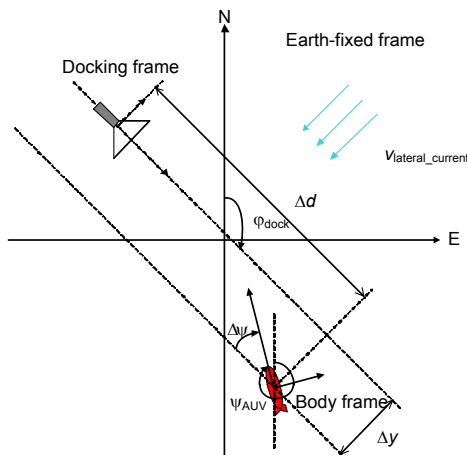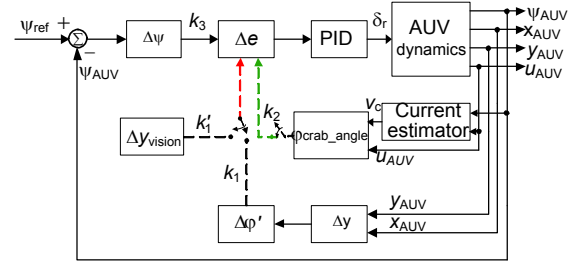

Fig. 7 Horizontal plane docking control loop

current velocity is further considered in the current compensation controller with $k_2 \neq 0$ in Eq. (1). If there is no current compensation term, cross-track errors will increase due to the current effect. Thus, current compensation is quite necessary for keeping the vehicle running along the dock cone centerline. The current estimator will be discussed in detail in Section 3.3.

In the terminal stage, vision information is used for navigation instead, for more accurate docking guidance. The term $\Delta\varphi'$ in Eq. (1) is switched to be the vision information $\Delta\varphi_{vision}$ in Fig. 7. Note that under the MOOS framework, it is quite flexible in switching or adding external items in the controller.

3.2 Current compensator design

To maintain the vehicle at a desired course in the presence of lateral currents, a crab angle correction term is introduced to the docking control loop in Eq. (1). The crab angle varies with the lateral current velocity and the AUV's velocity. In this subsection, we focus on horizontal crab angle calculation.

The crab angle is defined in Eq. (3). When the AUV is running in a steady state, which means the cross-track error Δy varies within δy during a certain time interval T, the input of the inner control loop Δe will approach zero. δy is a small value dependent on the cross-track error control accuracy.

If there is no lateral current, $\varphi_{crab\text{-}angle} = 0$. Because no current needs to be compensated, the final cross angle $\Delta\psi$ will be zero when the AUV runs in a steady state. As a result, the vehicle is expected to navigate along the cone centerline with a perfectly aligned heading.

If there exists lateral current, without crab angle correction, there will be a large constant cross-track error and a cross angle when the AUV is in a steady state. The path and attitude of the AUV running in this

Fig. 6 Angle and reference frame definitions

case are shown in red in Fig. 8. Since Δe is approximately zero when the AUV is in steady state, according to Eq. (1), there must be some non-zero cross angle $\Delta\psi$ to cancel the effect of the lateral current. Thus, the equivalent angle of the cross-track error and the cross angle in the steady state are related by

$$\Delta\varphi' = -\frac{k_3}{k_1}\Delta\psi, \qquad (4)$$

$$\Delta\psi = \arctan\left(\frac{v_{\text{lateral\_currents}}}{v_{\text{total}}}\right). \qquad (5)$$

With a crab angle term added as in Eq. (3), the steady cross angle is equal to the crab angle with $k_2 = k_3$ according to Eq. (1). Again, in the steady running state, the cross-track error and cross angle can be described as follows:

$$\Delta y = 0, \qquad (6)$$

$$\Delta\psi = -\varphi_{\text{crab\_angle}} = \arctan\left(\frac{v_{\text{lateral\_currents}}}{v_{\text{total}}}\right), \qquad (7)$$

and thus the AUV will track the cone centerline with a non-zero cross angle.

If crab angle correction is not accurate in Eq. (3), the cross-track error may not be zero, but should be less than the case without crab angle correction.

3.3 Online current estimation

According to the control strategy described above, the lateral current velocity in the docking frame should be obtained first for further current compensation. Most DVL systems (if not all) are able to measure both the velocities relative to the ground and the water column, and current velocity can be obtained as the subtraction of the two measured velocities. However, according to the DVL working principle, there is a minimum range for water tracking to guarantee adequate acoustic isolation; in addition, there exists a maximum altitude for bottom tracking to ensure enough echo intensity of the acoustic pulse. For the Explorer DVL we use, the minimum range for water profiling is 1 m, while the maximum altitude for bottom tracking is 60 m; the parameters may change with water quality. Strictly speaking, the current velocity measured by DVL is not the current around the vehicle but around the tracked water layer, and thus

the current velocity around the vehicle can hardly be accurately measured by DVL. Besides, the DVL with water tracking functions is always expensive. For the above reasons, we have to develop a current estimation algorithm for current compensation.

A novel current estimator is designed in addition to the docking controllers. The following current estimator can estimate the velocities of both horizontal and vertical current components, using only the measurement of AUV velocity relative to the ground.

3.3.1 Horizontal current estimator

In Fig. 8, the yellow AUV shows the vehicle's path and attitudes without current disturbances, and the red AUV is the one under current disturbances. Clearly, there exists a cross-track error Δy and cross angle $\Delta\psi$ induced by the lateral current.
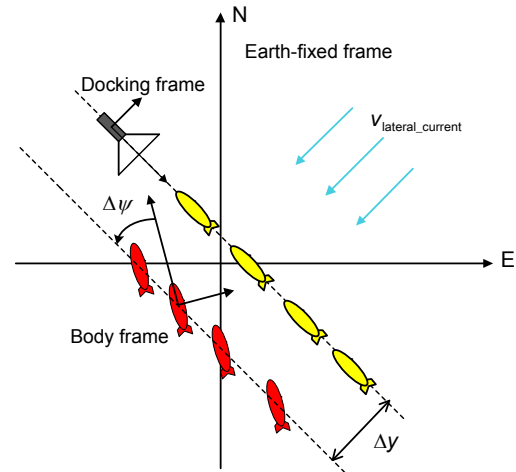

Fig. 8 Current effect analysis

We assume that the current is uniform and steady. When the AUV runs in a steady state, the cross-track error Δy will stay at a constant value, and thus the total velocity of the AUV will be parallel with the docking centerline. At this time, the input of the PID controller Δe is approximately zero, and the output is also around zero, which means that the deflection angles of the control planes are zero. For an under-actuated AUV, the lateral velocity of the AUV can be neglected in this case. The velocity relative to ground presented in the docking frame can be measured from DVL. From Fig. 8, we can obtain the following equation based on the AUV kinematics in Eq. (5):

$$v_{\text{lateral\_currents}} = v_{\text{total}} \tan(\Delta\psi). \qquad (8)$$

The above current estimator needs only the measurement of AUV's velocity relative to the ground, without using the one of the vehicle's velocity relative to the water column. If the output of the heading PID is not zero, which means that the control planes have certain deflection angles, the lateral body velocity of the AUV may not be neglected. The deflection of the control planes produces forces and moments that may affect the results of current estimation. According to Fossen (1994) and McEwen et al. (2008), Eq. (8) can be approximately modified as follows:

$$v_{\text{lateral\_currents}} = v_{\text{total}} \tan(\Delta\psi) + k(n)\delta_{\text{r}}, \qquad (9)$$

where δ_{r} is the deflection angle of the rudder (vertical control plane), n is the propeller speed (revolutions per minute), and $k(n)$ is a parameter factor related to the propeller speed, which needs to be calibrated. The second term on the right in Eq. (9) can be considered as the estimated lateral velocity of the AUV in the body frame, induced by rudder deflection. When the AUV is in a steady state in the docking process, the lateral current can be estimated by Eq. (9). However, in practice both $\Delta\psi$ and v_{total} are measured with errors:

$$\Delta\psi_{\text{measure}} = \Delta\psi + \xi_{\text{heading}}, \qquad (10)$$

$$v_{\text{measure}} = v_{\text{total}} + \xi_{\text{velocity}}, \qquad (11)$$

where $\Delta\psi_{\text{measure}}$ is the measured cross angle, v_{measure} is the measured vehicle velocity relative to the ground, ξ_{heading} describes the heading variation, including both measurement and control errors, and ξ_{velocity} is the measurement error of AUV velocity. The measured current can then be expressed as

$$\hat{v}_{\text{lateral\_currents}} = v_{\text{measure}} \tan(\Delta\psi_{\text{measure}}) + k(n)\delta_{\text{r}}. \qquad (12)$$

When the AUV is in a steady state, one can just calculate the mean value of $\hat{v}_{\text{lateral\_currents}}$ and then use it to estimate the lateral current. In practice, often the current is not uniform but varies slowly, and thus $\Delta\psi_{\text{measure}}$ may vary slowly; in this case, some sequential filtering, such as a Kalman-type filter, can be applied to estimate the horizontal current velocity.

3.3.2 Vertical current estimator

The vertical current can also influence the docking process. Estimation of the vertical current is similar to that of the horizontal one, but not the same since the AUV is asymmetrical with respect to the horizontal plane. In addition, there exists net buoyancy for safety, which also affects current estimation.

When the AUV is in a steady state in a constant-depth mission, the pitch of the AUV is a constant. Thus, the vertical current can be expressed as follows:

$$v_{\text{vertical\_currents}} = v_{\text{total}} \tan(\Delta\theta) + k'(n)\delta_{\text{e}}, \qquad (13)$$

where δ_{e} is the deflection angle of the elevator (horizontal control plane), $\Delta\theta$ is the pitch angle, and the other parameters have already been defined. The second term on the right in Eq. (13) is considered as the vertical velocity of the AUV in the body frame, induced by elevator deflection.

Again, $\Delta\theta$ and v_{total} may not be constant in practice, and they can be described as follows:

$$\Delta\theta_{\text{measure}} = \Delta\theta + \xi_{\text{pitch}}, \qquad (14)$$

$$v_{\text{measure}} = v_{\text{total}} + \xi_{\text{velocity}}, \qquad (15)$$

where $\Delta\theta_{\text{measure}}$ is the measured pitch, v_{measure} is the measured vehicle velocity relative to the ground, ξ_{pitch} describes the pitch variation, including both the measurement and control errors, and ξ_{velocity} is the measurement error of AUV velocity. Hence, the measured current can be written as

$$\hat{v}_{\text{vertical\_currents}} = v_{\text{measure}} \tan(\Delta\theta_{\text{measure}}) + k'(n)\delta_{\text{e}}. \qquad (16)$$

Similarly, we can just calculate the mean value of $\hat{v}_{\text{vertical\_currents}}$ when the AUV is in a steady state and then estimate the vertical current. Similar to the horizontal plane, some sequential filtering can be applied to estimate the vertical current velocity if the current varies slowly.

In this study, the vertical current is estimated and used as the trigger of the protection program. If the vertical current is too large, the depth control may be unstable. In this case, the AUV should end its docking attempt.

4 Simulation performance

Our simulation is run based on MOOS-IvP architecture as described in Section 2. The vehicle simulation incorporates a full six-degree-of-freedom (6-DOF) vehicle model replete with vehicle dynamics, center of buoyancy/center of gravity geometry, and velocity dependent drag (Newman, 2008). The controller described in Fig. 7 is implemented in the MOOS simulator. The mass of the AUV is 70 kg and the length is 2.5 m in our simulation model.

The docking process is studied using the control strategy and docking sequences developed in this study. We assume that the environment has a flat bottom with a depth of 20 m. The dock station is located at (0, 0, 20) m, and its orientation is 270°. The radius of the dock is 0.6 m, and the cone angle is 70°. The start point of the AUV is set at (−60, 10) m with an initial heading of 90°, and we set the velocity of the AUV to be 1 m/s in the simulation. Before the docking operation, the current is estimated using the method discussed in Section 3.3. All variables are represented in the Earth-fixed frame.

4.1 Current estimator performance

For current estimation simulation, we add lateral and vertical currents to the 6-DOF vehicle model in the simulator, and make the AUV conduct a docking process with cross-track error control.

4.1.1 In the horizontal plane

First we add respectively 0, −0.1, −0.2, −0.3, −0.4, and −0.5 m/s lateral currents and zero vertical current in the simulator, and estimate the current velocity using Eq. (9). The parameter k in Eq. (9) is pre-calibrated by selecting a special AUV speed and a special velocity of the current. Once the parameter is tuned at a certain propeller speed, it does not change further; however, if the propeller speed is changed from n to m, then the parameter k can be approximately described by mk/n. Fig. 9 shows the rudder's deflection angles when the vehicle runs through no current and −0.5 m/s current, respectively. From the figure, we find that the rudder's deflection angle is approximately zero even if there exists some current.

Table 1 shows the estimated lateral current velocities in the dock frame under different conditions, where the current is calculated by averaging the measured lateral current when the AUV is in steady state. From Table 1, we find that the current estimator can estimate the lateral current velocity accurately and effectively. The accuracy of the estimates meets our requirements for successful docking operations.
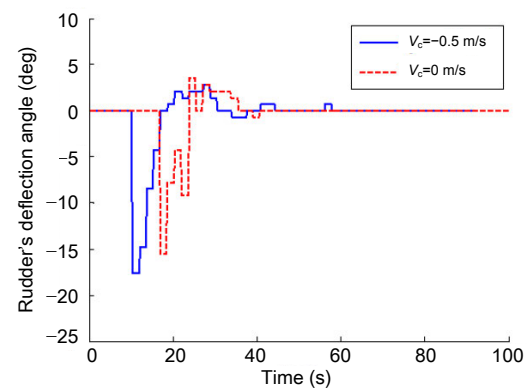

Fig. 9 AUV rudder's deflection angles in the docking process

Table 1 Lateral current estimation results

Case	True value (m/s)	Estimated value (m/s)	Estimated error (m/s)		Error percentage
			Bias	Standard deviation	
1	0	0	0	0.0007	−
2	−0.1	−0.1004	0.0004	0.0008	−0.416%
3	−0.2	−0.2004	0.0004	0.0007	−0.194%
4	−0.3	−0.3004	0.0004	0.0006	−0.142%
5	−0.4	−0.4009	0.0009	0.0008	−0.224%
6	−0.5	−0.5015	0.00015	0.0011	−0.293%

A Kalman filter (KF) is used for online current estimation. As shown in Eqs. (9)–(12), the measurement noise is dependent on the heading control accuracy, so we set the process error as $\omega \sim N(0, 0.05^2)$, and the measurement noise as $v \sim N(0, 1)$. Fig. 10 shows the estimated current speed versus time when a current of −0.5 m/s is considered. The blue line is the true current velocity, and the red curve is the estimated one. At the beginning, the AUV is not steady, and the estimated current velocity fluctuates because of the heading variation. When the AUV is in a steady state, the current estimate converges as close as the true current.

4.1.2 In the vertical plane

To validate the performance of vertical current estimation, we add 0, −0.1, −0.2, −0.3, −0.4, and −0.5

m/s vertical currents, respectively, and no lateral current in the simulation model. Also, we add 1 N net buoyancy in the AUV model for practical purposes.
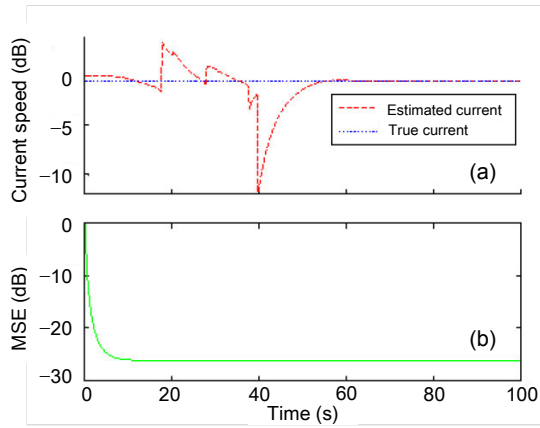

Fig. 10 Current estimation results: (a) estimation of currents speed; (b) estimation error covariance

Similar to the parameter k in Eq. (9), the parameter k' in Eq. (13) needs to be pre-calibrated by selecting a special AUV speed and a special velocity of the current. Because of the asymmetry of the AUV body and the presence of net buoyancy in the vertical plane, the elevator's deflection angles oscillate around a non-zero constant when the AUV is in steady state (Fig. 11). Table 2 shows the estimation results under different conditions, where the current is calculated by averaging the measured vertical current when the AUV is in steady state. From Table 2, it can be found that the current estimator can estimate the vertical current effectively in the presence of 1 N net buoyancy. Comparing the estimation results with the horizontal ones, we find that the latter has a better performance than the former. This is because the control accuracy in the horizontal plane is higher than the one in the vertical plane. KF is again used for online current estimation. As shown in Eqs. (13)–(16), the measurement noise is dependent on the pitch control accuracy, so again we set the process error as $\omega \sim N(0, 0.01^2)$ and the measurement noise as $v \sim N(0, 1)$. The estimation results are shown in Fig. 12. The blue line in the figure is the true current velocity, and the red curve is the estimated one. At the beginning, the AUV is not yet steady, and the estimated current velocity is far away from the true value. When the AUV is in a steady state, the current estimate converges to the true value but with a small fluctuation.

The pitch is limited to [−25°, 25°] in our simulation for stability considerations. The AUV does not approach the steady state at the first 90 s since the depth changes at that time. This leads to the disagreement between the red and blue curves in Fig. 12.
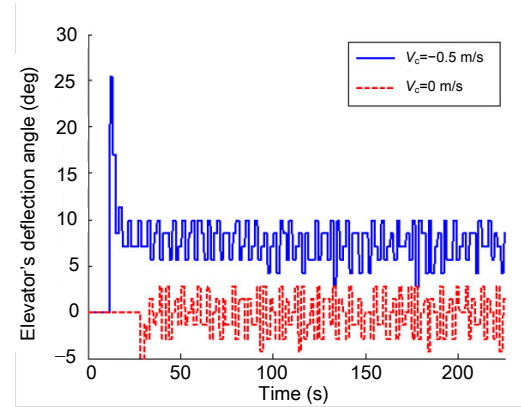

Fig. 11 AUV elevator's deflection angles in the docking process with 1 N net buoyancy

Table 2 Vertical current estimation results

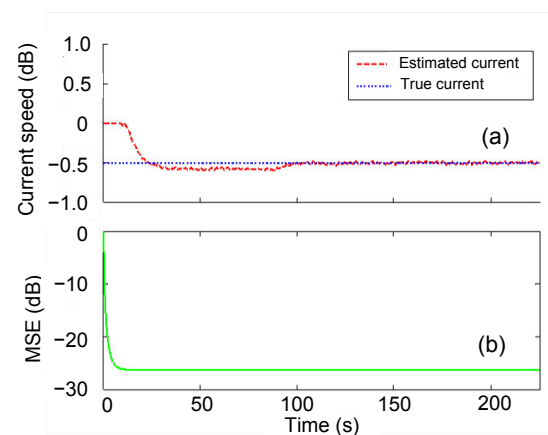| Case	True value (m/s)	Estimated value (m/s)	Estimator error (m/s)		Error percentage
			Bias	Standard deviation	
1	0	0.0000	0.0000	0.0631	–
2	−0.1	−0.0997	−0.0003	0.0620	0.302%
3	−0.2	−0.2013	0.0013	0.0593	−0.661%
4	−0.3	−0.3011	0.0011	0.0539	−0.370%
5	−0.4	−0.4013	0.0013	0.0554	−0.322%
6	−0.5	−0.5014	0.0014	0.1003	−0.280%

Fig. 12 Estimation results of the vertical current with 1 N AUV net buoyancy: (a) estimate of current speed; (b) estimation error covariance

The above simulations show that the developed current estimator can evaluate both horizontal and vertical components of current velocity, using only the measurement of AUV's velocity relative to the ground. The controlled attitudes are critical for this current estimator to work properly. Comparatively, lateral current estimation is more effective and simple, which is very important for docking operation; however, the behavior of the vertical current estimator is more complicated because of body asymmetry and net buoyancy. The parameter k needs to be calibrated previously by experiments for a certain type and speed of AUV in practice. Most importantly, in this study the current can be estimated online during a docking process via KF.

4.2 Docking control simulation

Using the control strategy developed in the previous sections, here we study cross-track error control under the disturbance of different lateral currents. Again, the AUV starting point is set at (−60, 10) m in the dock frame.

It is better to guide the AUV to track a predefined path for docking operation. Commonly, the AUV should first go to the centerline of the cone and then approach the dock. A successful docking attempt requires the following two basic conditions (in the horizontal plane):

1. The cross-track error is less than the radius of the dock (0.6 m in this work).

2. The cross angle between AUV heading and the cone axis is less than a certain value (35° in this work).

Case 1: cross-track error control with no current

We assume there is no lateral current, and the AUV starts docking with cross-track error control and heading control, which means k_2 is zero in Eq. (1). Fig. 13 presents the results, where the green dot curve is the AUV trajectory, the red arrow is the AUV heading, the blue star is the start point, and the blue triangle is the dock station. The results show that the control method can eliminate the cross-track error with no current, and also make the cross angle approach zero, as expected. In this case, the AUV can get into the dock successfully.

Case 2: cross-track error control in current without current compensation

We assume that there exists a lateral current, but that the AUV implements docking operation without

current compensation, which means k_2 is still zero in Eq. (1). We compare the control results in currents with the speed equal to 0, −0.1, −0.3, and −0.5 m/s, respectively. As shown in Fig. 14, without current compensation, the controller cannot eliminate the cross-track error, and the larger the current velocity, the larger the cross-track error. From Fig. 14, we can see that the cross angle is not zero in currents, and that the larger the current velocity, the larger the cross angle. The cross-track error and cross angle turn to be constant when the AUV is in a steady state. However, the results show that the vehicle fails to enter the dock entrance according to the given requirements on motion control.
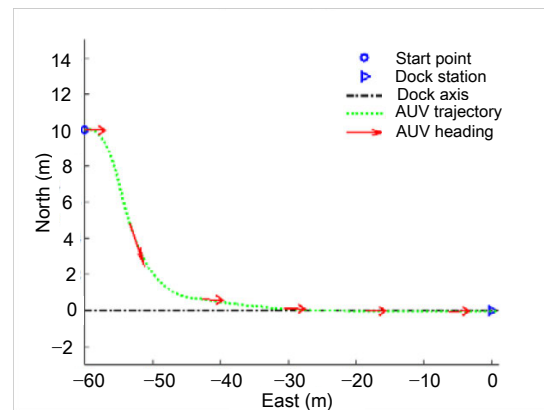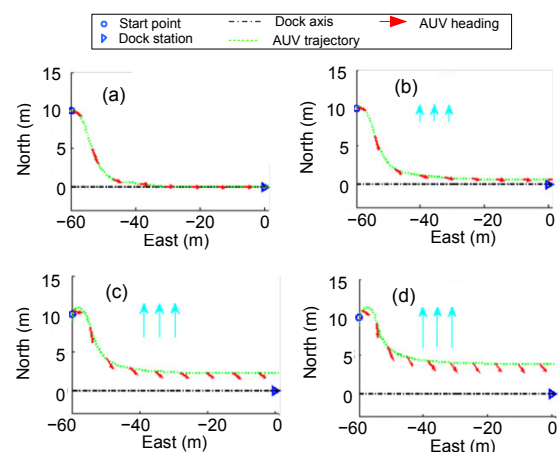

Fig. 13 Simulation results in case 1

Fig. 14 Simulation results in case 2 under different current conditions: (a) V_c=0 m/s; (b) V_c=−0.1 m/s; (c) V_c=−0.3 m/s; (d) V_c=−0.5 m/s

Case 3: cross-track error control in current with current compensation

We assume that there exist lateral currents, and that the AUV implements docking operation with

current compensation, which means k_1, k_2, and k_3 are all non-zero in Eq. (1); we set $k_1=k_2=k_3=1$. The current is estimated and compensated in the docking control loops. Again, we compare the control results in different currents with the speed equal to 0, −0.1, −0.3, and −0.5 m/s, respectively. As shown in Fig. 15, with current compensation, the controller can eliminate the cross-track error very well even in the presence of a lateral current. From Fig. 15, we can also see that the cross angle is non-zero in current, and that the larger the current velocity, the larger the cross angle. The cross angle turns to be constant when the AUV is in steady state. The cross-track error and cross angle are controlled to meet the requirements for a successful docking operation.
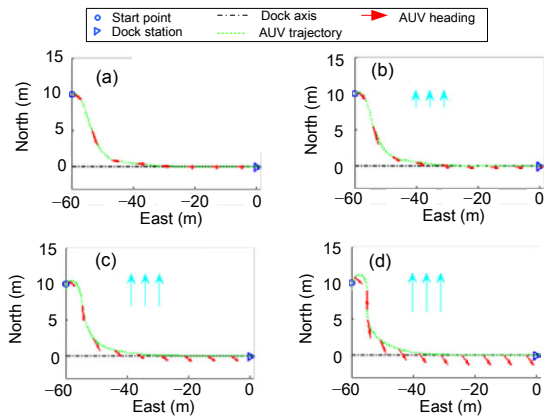

Fig. 15 Simulation results in case 3 under different current conditions: (a) $V_c=0$ m/s; (b) $V_c=−0.1$ m/s; (c) $V_c=−0.3$ m/s; (d) $V_c=−0.5$ m/s

As a conclusion, without current compensation, the cross-track error may be large for docking (Fig. 14). Part of the reason is that the gain of the path-following controller is not large enough to resist the current. If the gain of the path-following controller is set large enough, the cross-track error may become smaller. However, increasing the gain of the path-following controller and ensuring the stability of the control system require tuning the control parameters carefully, which is quite time-consuming and less effective. Actually, the main reason for the fluctuation of the cross-track error is that the forward speed is not large enough to provide enough thrust, while increasing the forward speed can improve the AUV's capability in resisting current disturbance. However, large speed could also make the AUV hit

the dock station heavily with too much force at the docking point. In our proposed path-following strategy, the AUV is able to dock at a reasonable speed and the control parameters are easily tuned. According to the results of our lake experiments and preliminary sea trials, the AUV's forward speed set to be 1 m/s works well in the docking operations.

5 Experimental results

To validate the performance of the proposed current estimation/compensation algorithm and the docking system, sea trials were conducted separately in April and May, 2017, in the South China Sea. The sea tests in April were conducted to validate the effectiveness of the AUV current estimator/compensator without locating the dock station in the field, while the further sea trials in May were conducted to test the whole docking system.

5.1 Sea tests of the current estimator/compensator

To evaluate the performance of the current estimator/compensator, a series of sea tests were carried out in the South China Sea (Fig. 16).

Fig. 16 Sea test for the current estimator/compensator

The selected sea area has a relative flat bottom with a depth of about 30 m. We validated the current estimator and also compared AUV docking control performance with and without the current compensator. To ensure a better performance of DVL, the AUV was set to dive to the depth of 10 m underwater. The AUV uses EKF for navigation data filtering in underwater missions without USBL.

5.1.1 Current estimation

First, the AUV ran a docking attempt to a virtual dock station at the speed of 1 m/s with cross-track

error control on surface, and then dove to 10 m water depth to perform docking operation. The virtual dock station was assumed to be located at the given position, like (−94, 35) m in the horizontal plane, with the orientation at 290°. Fig. 17 shows the estimated lateral current speeds expressed in the dock frame, which are processed by KF with a process error of $\omega \sim N(0, 0.01)$, and a measurement noise of $v \sim N(0, 0.1)$. The red curves in the figures are the estimated current velocities, and the blue dot curves are the current velocities measured by DVL. Fig. 17 shows that the current estimates can converge to the DVL-measured current velocities in fewer than 10 s. Note that there is more noise in the estimated current speed in Fig. 17a because of surface wave disturbances. Overall, the results demonstrate that the proposed current estimation method is feasible and effective under reasonable current conditions.

5.1.2 AUV docking operation in currents

Since the online current estimation algorithm has been validated effectively, the proposed current compensator can be further applied in the control algorithm. The control algorithm was tested separately without locating the dock station in the field; thus, a virtual dock station was assumed to be located at (−94, 35, 10) m, with the orientation at 290°. There were no USBL or vision systems applied during the experiments; we adopted autonomous navigation devices combined with EKF for navigation data filtering. The effectiveness of the control algorithm was evaluated by the final cross-track errors and the cross angle at the dock station.

Tests were conducted with and without the current compensator. The AUV was run with the control algorithm, and the AUV's speed was set to be 1 m/s during the tests. The forward speed controller employed in this study is the conventional PID loops, and the control results are shown in Fig. 18. Since there is nothing special in the PID controllers themselves, here we just omit the specific details of the controllers to shorten this paper.

The corresponding current velocity during the docking operation is shown in Fig. 17b. Fig. 19 shows the comparison results for the following two scenarios:

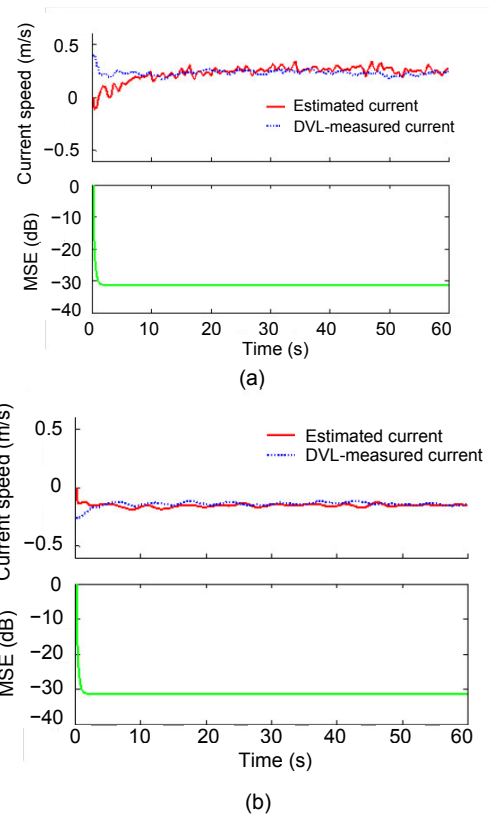1. AUV docking without current compensation (red dot curve);

Fig. 17 Current estimation results in sea tests: (a) current estimation results on the surface; (b) current estimation results in a depth of 10 m
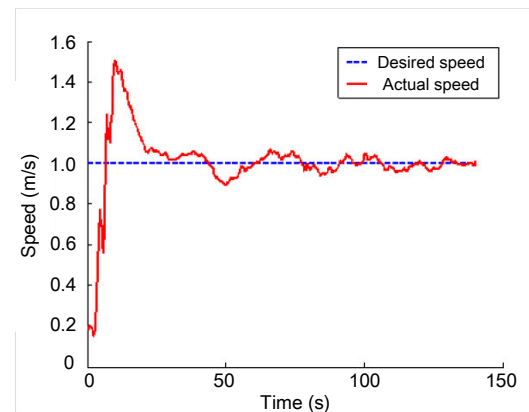

Fig. 18 Forward speed of the AUV in the field experiments

2. AUV docking with current compensation (green double dot curve).

Fig. 19a gives the AUV paths during the docking operation. As stated in Section 3, a successful docking operation is achieved if the final cross-track error and cross angle are less than 0.6 m and 35°, respectively.
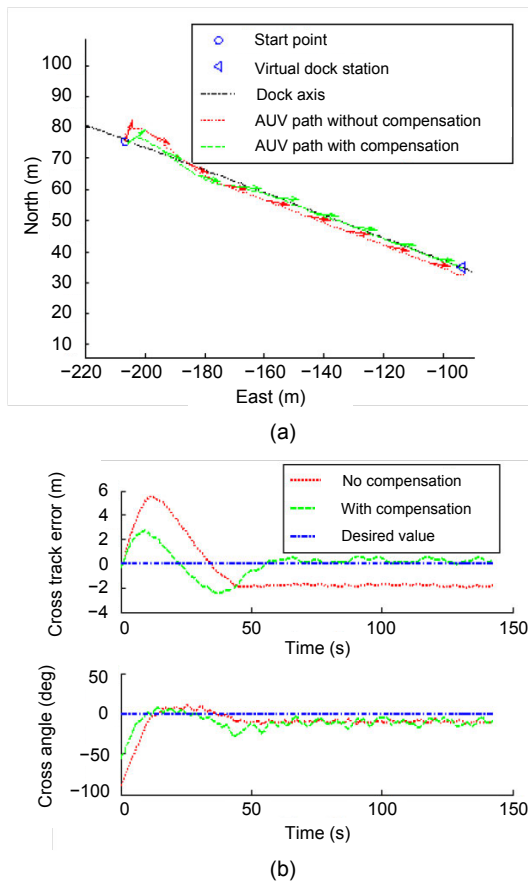
(a)

(b)

Fig. 19 Docking experimental results in currents with or without compensation: (a) vehicle track; (b) corresponding cross-track error and cross angle

Fig. 19b shows that without current compensation, the final cross-track error is too large to achieve a successful docking operation. However, the cross-track error is sufficiently restrained with current compensation, as shown by the green curve in Fig. 19. The cross-track error and cross angle here are defined and expressed in the dock frame.

Comparing the two cases, it can be found that with current compensation, the cross-track error can be kept within the required range to achieve a successful docking operation, even though the fluctuation of the cross-track error and the cross angle are more obvious than the case without compensation (Fig. 19b).

5.2 Sea trials of the docking system

To test the docking system and the control strategy, a series of sea trials was carried out in the South China Sea in May, 2017. The whole docking

system was tested in the sea areas with water depth of about 50 m and 105 m, respectively.

First, we tested the docking system at the water depth of 50 m (Fig. 20). The dock station was deployed and located on the sea bottom. The docking and undocking strategy shown in Figs. 4 and 5 had been fully implemented and validated with the vehicle. During the sea trials, the dock station was positioned at (0, 0, 50) m, and the dock orientation was fixed at 330°.

Fig. 20 Sea test for docking

We conducted 10 runs of successful docking operation at 50 m water depth. Fig. 21 gives the experimental results of one successful underwater docking attempt. The vehicle initiated the docking operation at a start point on the water surface. When the AUV approached close enough to a certain point on the surface, which was located in front of the dock station, the vehicle started to dive; if the depth of the AUV is close to the dock station, it began homing and searching for a USBL signal. Once the AUV got a USBL position fix, it began to approach a given point which was located on the dock centerline but 150 m away from the dock station. Fig. 21a shows the docking trajectory of the AUV from the start point on the surface to the dock station underwater. We can see that the vehicle passed by the marked point, accurately followed the dock centerline and finally entered the dock entrance. Figs. 21b and 21d present the corresponding cross-track error and cross angle, respectively. Fig. 21c gives the depths of the AUV and the dock station. According to Fig. 21, it can be found that the AUV cross-track error is less than 0.6 m, the depth error is less than 0.6 m, and the cross angle is less than 35° when the vehicle docks with the dock station. This illustrates that a successful docking operation is achieved. There was a small jump in the
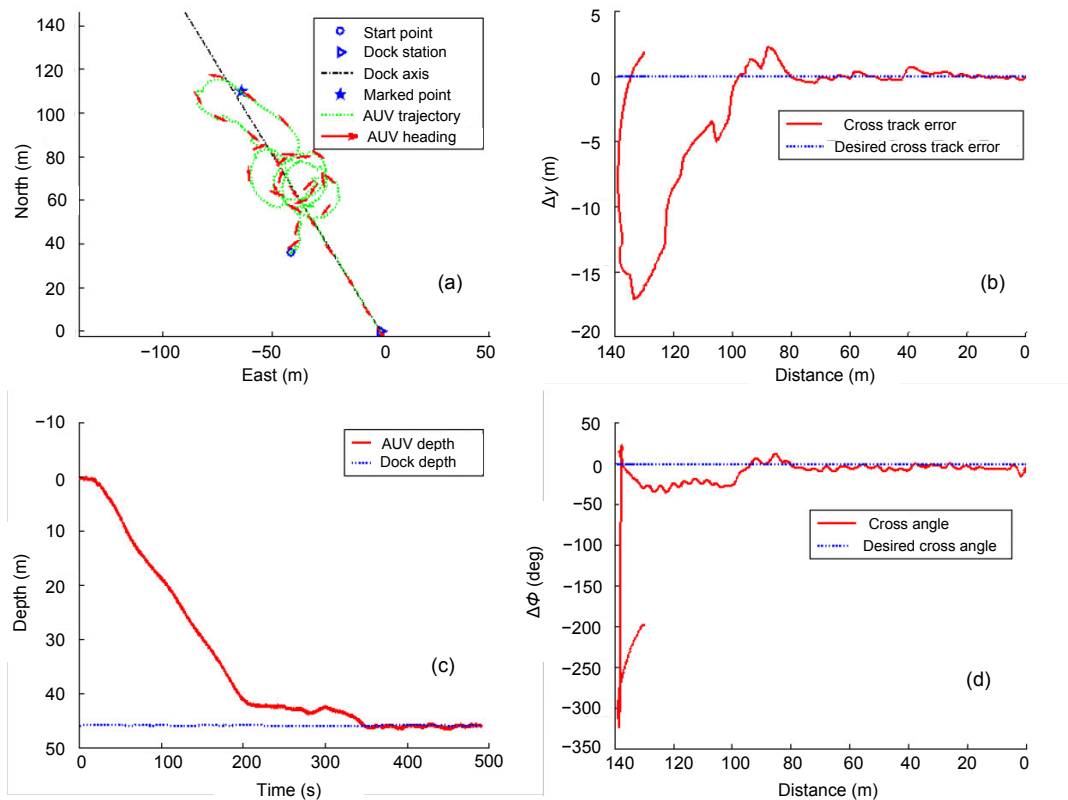
Fig. 21 One successful docking trial in depth of 50 m: (a) AUV track in docking process; (b) cross-track error; (c) depths of the AUV and the dock station; (d) cross angle

cross angle when the vehicle ran near the dock station. This is because the AUV hits the funnel-shaped dock entrance, which channeled the vehicle into the terminal tube and caused the change on the vehicle's heading.

As seen from Fig. 21a, the small fluctuation along the trajectory is induced by the less stableUSBL position fixes. The accuracy of USBL navigation is good enough to navigate the AUV near the dock station. However, it is not accurate enough for terminal docking operation. The vision guidance was applied in the terminal stage. From the sea tests, we can see that our navigation/guidance and control systems are robust and accurate enough to make a successful docking operation.

The lateral and vertical current velocities in the experimental sites are presented in Fig. 22. The red curve shows lateral current velocity, while the blue curve presents vertical current velocity. Fig. 22 shows that there existed obvious lateral current during the experiments, and thus current compensation is necessary for motion control in the horizontal plane.
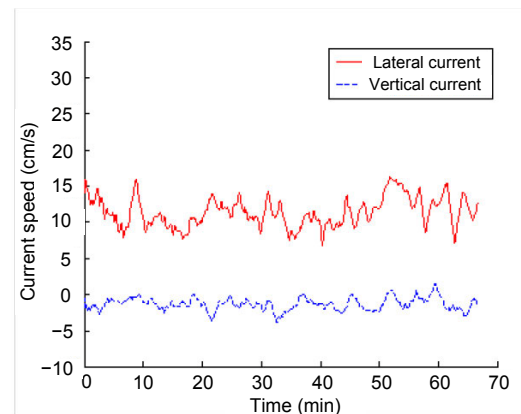

Fig. 22 Current in the experimental sites

Once the AUV was latched inside the dock station, it started to charge the battery, upload the collected data, and download the next commands. Once a new mission was uploaded, the AUV began to undock by reversing the propeller. When the AUV moved backward far away from the dock station, the undocking process was ended, and the AUV started to

execute the new mission. Fig. 23 shows the undock trajectory, from which it can be found that the AUV can undock successfully.
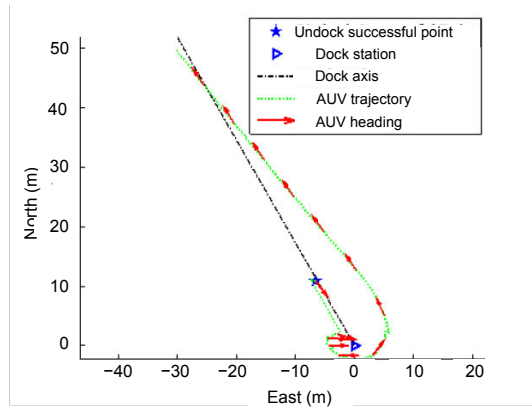

Fig. 23 One successful undocking trial in a depth of 50 m

After the docking system was fully tested at 50 m water depth, the dock station was further deployed at the depth of 105 m to test the robustness of the docking system. During this set of tests, the dock station was positioned at (0, 0, 105) m, and the dock orientation was 20.8°. Similar to the previous experiments, the whole docking and undocking operations were conducted. The AUV entered the dock station successfully. The power charging and data transmission functions were also validated when the AUV was latched inside the dock station.

Our control strategy was fully tested and validated with a series of field trials. As shown in Fig. 21, the proposed control methods can keep the cross-track error and cross angle within the required ranges in the open sea environments, which illustrates the feasibility and robustness of our control algorithm and docking system. The docking scheme shown in Figs. 4 and 5 proves effective for underwater docking operation, and it is especially suitable for the given type of docking AUV and docking station.

6 Conclusion and future work

In this paper, a prototype underwater docking system is designed, including the dock station, docking AUV, and docking algorithms. A novel control approach that can handle current disturbances via online current estimation/compensation is presented.

Different from the traditional current estimator, in which the AUV's velocity relative to both the ground and the water column are needed, the proposed method just needs the measurement of the AUV's velocity relative to the ground to estimate the current velocity. Through the simulations based on the MOOS-IvP model, the control strategy and the current estimator/compensator are thoroughly analyzed and verified. Moreover, the docking process, control strategy and current estimator/compensator are fully implemented in our docking system. Sea trials were carried out in the South China Sea at different depths. Sea trial results validated the feasibility and effectiveness of the proposed control strategy and current estimator/compensator. The docking scheme proved robust and effective in the sea tests. Our docking system showed satisfactory performance when docking the vehicle to the station.

Future work will be focused on the improvement of the guidance and control algorithms. As the velocity of the lateral current increases, the current compensation method may lose its effectiveness, and this means the cross angle and the cross-track error are both too large to achieve successful docking operations. In this case, a different docking path should be planned to align the AUV's heading with the docking heading in a large current; the docking path may be designed depending on the current information.

References

Allen B, Austin T, Forrester N, et al., 2006. Autonomous docking demonstrations with enhanced REMUS technology. *OCEANS*, p.1-6.
https://doi.org/10.1109/oceans.2006.306952

Baumgartner MF, Stafford KM, Winsor P, et al., 2014. Glider-based passive acoustic monitoring in the Arctic. *Mar Technol Soc J*, 48(5):40-51.
https://doi.org/10.4031/MTSJ.48.5.2

Borgogna G, Lamberti T, Massardo AF, 2015. Innovative power system for autonomous underwater vehicle. *OCEANS*, p.1-8.
https://doi.org/10.1109/oceans-genova.2015.7271339

Bradley AM, Feezor MD, Singh H, et al., 2001. Power systems for autonomous underwater vehicles. *IEEE J Ocean Eng*, 26(4):526-538. https://doi.org/10.1109/48.972089

Chen YH, Yang CJ, Li DJ, et al., 2012a. Design and application of a junction box for cabled ocean observatories. *Mar Technol Soc J*, 46(3):50-63.
https://doi.org/10.4031/MTSJ.46.3.4

Chen YH, Yang CJ, Li DJ, et al., 2012b. Development of a direct current power system for a multi-node cabled ocean observatory system. *J Zhejiang Univ-Sci C (Comput & Electron)*, 13(8):613-623.
https://doi.org/10.1631/jzus.C1100381

Choyekh M, Kato N, Short T, et al., 2015. Vertical water column survey in the Gulf of Mexico using autonomous underwater vehicle SOTAB-I. *Mar Technol Soc J*, 49(3): 88-101. https://doi.org/10.4031/MTSJ.49.3.8

Cowen S, Briest S, Dombrowski J, 1997. Underwater docking of autonomous undersea vehicles using optical terminal guidance. MTS/IEEE Conf Proc, p.1143-1147.
https://doi.org/10.1109/oceans.1997.624153

Curtin TB, Bellingham JG, Catipovic J, et al., 1993. Autonomous oceanographic sampling networks. *Oceanography*, 6(3):86-94. https://doi.org/10.5670/oceanog.1993.03

Fossen TI, 1994. Guidance and Control of Ocean Vehicles. John Wiley & Sons Inc., New York, USA, p.89-90.

Kilgour MJ, Auster PJ, Packer D, et al., 2014. Use of AUVs to inform management of deep-sea corals. *Mar Technol Soc J*, 48(1):21-27. https://doi.org/10.4031/MTSJ.48.1.2

Li B, Xu YX, Liu CZ, et al., 2014. Simulation and preliminary experimental results on S-surface control of an autonomous underwater vehicle based on MOOS-IvP. OCEANS, p.1-6. https://doi.org/10.1109/oceans.2014.7003168

Li B, Xu YX, Liu CZ, et al., 2015. Terminal navigation and control for docking an underactuated Autonomous Underwater Vehicle. Proc IEEE Int Conf on Cyber Technology in Automation, Control, and Intelligent Systems, p.25-30. https://doi.org/10.1109/cyber.2015.7287904

Li DJ, Chen YH, Shi JG, et al., 2015. Autonomous Underwater Vehicle docking system for cabled ocean observatory network. *Ocean Eng*, 109:127-134.
https://doi.org/10.1016/j.oceaneng.2015.08.029

Li ZS, Li DJ, Lin L, et al., 2010. Design considerations for electromagnetic couplers in contactless power transmission systems for deep-sea applications. *J Zhejiang Univ-Sci C (Comput & Electron)*, 11(10):824-834.
https://doi.org/10.1631/jzus.C0910711

Ludvigsen M, Johnsen G, Sørensen AJ, et al., 2014. Scientific operations combining ROV and AUV in the Trondheim Fjord. *Mar Technol Soc J*, 48(2):59-71.
https://doi.org/10.4031/MTSJ.48.2.3

McEwen R S, Hobson B W, McBride L, et al., 2008. Docking control system for a 54-cm-diameter (21-in) AUV. *IEEE J Ocean Eng*, 33(4):550-562.
https://doi.org/10.1109/joe.2008.2005348

Newman P M, 2008. MOOS—Mission Orientated Operating Suite. Technical Report, 2299(08), Massachusetts Institute of Technology.

Park JY, Jun BH, Kim K, et al., 2009. Improvement of vision guided underwater docking for small AUV ISiMI. OCEANS, p.1-5.
https://doi.org/10.23919/OCEANS.2009.5422241

Park JY, Jun BH, Lee PM, et al., 2011a. Docking problem and guidance laws considering drift for an underactuated AUV. OCEANS, p.1-7.
https://doi.org/10.1109/oceans-spain.2011.6003574

Park JY, Jun BH, Lee PM, et al., 2011b. Modified linear terminal guidance for docking and a time-varying ocean current observer. Proc IEEE Symp on Underwater Technology (UT) and Workshop on Scientific Use of Submarine Cables and Related Technologies, p.1-6.
https://doi.org/10.1109/ut.2011.5774141

Peng SL, Yang CJ, Fan SS, et al., 2014. Hybrid underwater glider for underwater docking: Modeling and performance evaluation. *Mar Technol Soc J*, 48(6):112-124.
https://doi.org/10.4031/MTSJ.48.6.5

Refsnes JE, Pettersen KY, Sørensen AJ, 2006. Control of slender body underactuated AUVs with current estimation. Proc 45th IEEE Conf on Decision and Control, p.43-50. https://doi.org/10.1109/cdc.2006.376984

Sato Y, Maki T, Kume A, et al., 2014. Path replanning method for an AUV in natural hydrothermal vent fields: Toward 3D imaging of a hydrothermal chimney. *Mar Technol Soc J*, 48(3):104-114. https://doi.org/10.4031/MTSJ.48.3.5

Shi JG, Li DJ, Yang CJ, 2014. Design and analysis of an underwater inductive coupling power transfer system for autonomous underwater vehicle docking applications. *J Zhejiang Univ-Sci C (Comput & Electron)*, 15(1):51-62.
https://doi.org/10.1631/jzus.C1300171

Shi JG, Li DJ, Yang CJ, et al., 2015. Impact analysis during docking process of autonomous underwater vehicle. *J Zhejiang Univ (Eng Sci)*, 49(3):497-504 (in Chinese).
https://doi.org/10.3785/j.issn.1008-973X.2015.03.015

Singh H, Bellingham JG, Hover F, et al., 2001. Docking for an autonomous ocean sampling network. *IEEE J Ocean Eng*, 26(4):498-514. https://doi.org/10.1109/48.972084

Teo K, An E, Beaujean PPJ, 2012. A robust fuzzy autonomous underwater vehicle (AUV) docking approach for unknown current disturbances. *IEEE J Ocean Eng*, 37(2): 143-155. https://doi.org/10.1109/JOE.2011.2180058

Teo K, Goh B, Chai O K, 2015. Fuzzy docking guidance using augmented navigation system on an AUV. *IEEE J Ocean Eng*, 40(2):349-361.
https://doi.org/10.1109/JOE.2014.2312593

Xiang XB, Yu CY, Zhang Q, et al., 2016. Path-following control of an AUV: fully actuated versus under-actuated configuration. *Mar Technol Soc J*, 50(1):34-47.
https://doi.org/10.4031/MTSJ.50.1.4

Xie YC, Huang H, Hu Y, et al., 2016. Applications of advanced control methods in spacecrafts: progress, challenges, and future prospects. *Front Inform Technol Electron Eng*, 17(9):841-861. https://doi.org/10.1631/FITEE.1601063

Zhang M, Xu YX, Li B, et al., 2014. A modular autonomous underwater vehicle for environmental sampling: system design and preliminary experimental results. OCEANS, p.1-5. https://doi.org/10.1109/oceans-taipei.2014.6964495

Zhang M, Xu W, Xu YX, 2016. Inversion of the sound speed with radiated noise of an autonomous underwater vehicle in shallow water waveguides. *IEEE J Ocean Eng*, 41(1): 204-216. https://doi.org/10.1109/JOE.2015.2418172

Zhou JJ, Tang ZD, Zhang HH, et al., 2013. Spatial path following for AUVs using adaptive neural network controllers. *Math Prob Eng*, 2013:749689.
https://doi.org/10.1155/2013/749689